Ventricular Beat Detection and Classification in Long Term ECG Recordings

Stoyan Tanev

Aerospace Technique and Technology
Institute of Space Research and Technologies
Bulgarian Academy of Sciences
29 Acad. Georgi Bonchev Str.
Sofia 1113, Bulgaria
E-mail: spsbyte@space.bas.bg

*Corresponding author

Received: June 25, 2012 **Accepted: December 28, 2012**

Published: January 8, 2013

Abstract: *The QRS detection is key component of each automated ECG analysis. For this purpose a lot of QRS algorithms have been already developed. In the same time the number of new published methods continues to grow up. This implicitly proves the impossibility of building such detector that could totally cover the variety of all shapes of ventricular beats encountered in practice. Generally, limited studies on discrimination between normal (sinus) and ectopic beats are available.*

The paper describes very fast procedure for accurate QRS detection in long term ECG Holter recordings, followed by classification of the complexes in normal and ectopic. The algorithm was tested with the widely accepted AHA and MIT-BIH databases. The obtained sensitivity and specificity are comparable to other published results.

Keywords: *ECG, QRS detection, Ectopic beat detection, Ventricular beat classification.*

Introduction

Each automated ECG analysis begins with detection of the QRS complexes since the patterns of the ventricular depolarization normally are the most distinguishable waveforms in the signal. Then in case of morphological analysis, the other ECG waves also are identified and delineated. The amplitudes, widths, intervals and relationships between them are measured and compared to statistically created sets of data for classifying the heart activity as normal or pathological. The rhythm analysis is based on discrimination between normal (sinus) and ectopic ventricular beats, which are detected off-line in long term, usually 24 hours Holter recordings. Thus, the cardiologists obtain full information about possible rhythm disturbances, including the time of occurrence of pathological episodes with different in type and shape ectopic beats. Epochs of sinus QRS complexes are investigated for assessment of the RR interval variation.

Very often, the two classes of ventricular beats are discriminated at a second level with algorithm, which detects some ectopic beats that are missed by the first algorithm designed for investigation of all types of QRS complexes [12].

The early developed hardware and software approaches have been based on features extracted from first or second derivative of the ECG signal [2, 3, 20]. Because of the relatively low computational complexity, they continue to be often used in real or quasi-real time analysis as well as for investigation of long term recordings. Standard signal processing methods also are

applied, such as linear and nonlinear filtering [1, 35], threshold technique [6, 7, 15], feature extraction [13, 17, 25], wavelet transform [11, 19, 30, 31, 33], neural networks [14, 37], genetic algorithms [27], morphological approaches [34, 36], Hilbert transform [5], template-match technique [4, 22].

The preprocessing stage of a real time QRS detector, reported by Ruha et al. [29], includes signal attenuation outside the 0.5-35-Hz frequency band, comb filter with first zero at 50 Hz, and band-pass filtering from 15 through 40 Hz. Then the QRS complexes are detected by an adaptive threshold, tracking the 40% of the maximum signal value within the last 1.5 s interval. The threshold is hold at 90% during 200 ms after each detected ventricular beat to avoid false algorithm activation due to high amplitude T waves. The QRS detection performance is checked with records 103 and 105 from the MIT-BIH database [24] only.

The method proposed by Saurabh and Mitra [32] consists of power-line interference and drift suppression, peak correction based on information extracted from the noise, and signal squaring. Then each sharp central peak, which is part of three consecutive peaks, is associated with R wave of normal in shape QRS complexes. However, several sinus ventricular beats may include more peaks, e.g. the configuration RSR'S'. The sensitivity and the specificity of the method were compared with these obtained by four other authors using the MIT-BIH database. The calculated values differ slightly each other.

Darrington [10] combined known algorithm with a shifting window, thus obtaining high pass filtering in a pseudo real time behavior.

Das and Chakraborty [9] applied the Pan Tompkins' algorithm by using a Savitzky-Golay filter instead of the original high pass filter and differentiator. No results with some of the recognized databases are reported.

Kohler et al. [21] investigate the QRS complexes counting the number of zero crossings per segment of the ECG signal. They reported excellent performance of the algorithm confirmed by checking it over selected channel from each of the two-channel recordings taken from the MIT-BIH database. The authors found this method is robust against noise since the residual noise after band-pass filtering oscillates around zero, whereas the peaks of the QRS complex have higher amplitude.

Christov [7] compares the absolute values of one or more summed differentiated ECG leads to a threshold, which combines three parameters: an adaptive slew-rate value, a second value which rises with the occurrence of high-frequency noise, and a third one intended to avoid missing of low amplitude beats. This method for QRS detection was tested by the entire MIT-BIH database. The obtained sensitivity and specificity are higher than 99%. Later, the author extended the assessment over the AHA database that confirmed the workability of the algorithm [8].

The QRS detector reported by Haiying Zhou et al. [16] copes with noises, artifacts and morphology variation of the ECG signal by exploiting a self-adaptive method for optimum thresholding of estimated peaks within ECG sub-segments. The overall results show that the algorithm provides the same performance as the classical ones.

Portet et al. [28] evaluated the detection performance of four real time QRS detection algorithms. Recordings of 8 QRS morphologies were mixed with electrode motion artefact,

muscle artefact and physiological drift and used as input to the QRS detectors. The results obtained specify the algorithms as complementary, each of them being superior with some of the morphologies.

Another approach to QRS detection is based on error back propagation neural network [26]. The algorithm uses a modified slope feature obtained by transformation of the denoised ECG signal.

Mehta and Lingayat [23] used support vector machine for comparative study of QRS detection in single lead based on entropy and combined entropy criteria. The power-line interference and drift are suppressed by digital filtering techniques. Both algorithms performed highly effectively with the recordings of the CSE ECG database.

Combined criterion for QRS detection was developed by Dotsinsky and Stoyanov [13]. It is based on high amplitude, steep leading and/or trailing edges, and sharp peak of the current candidate. Two differences between the ongoing sample S_i and the adjacent samples S_{i-n} and S_{i+n} are calculated, where n is usually the sample number within one interference period. A peak is detected when both differences have the same sign. Then the unsigned sum $U_i = |2S_i - S_{i-n} - S_{i+n}|$ is compared with the adaptive threshold M and a QRS candidate is detected every time $U_i > M$. This procedure is part of algorithm for ventricular beat detection. Another branch of it considers the discrimination of the complexes in normal and ectopic taking in consideration the occurrence of biphasic waves and the ratio of two adjacent RR intervals. The authors obtained sensitivity and specificity of 99.28% and 99.58% for AHA database, and 98.68% and 99.69% for MIT-BIH database [24].

Krasteva and Jekova [22] reported a quasi-real time method for discrimination of ventricular ectopic beats from both supraventricular and paced beats. The maximal cross-correlation, the area difference and the frequency spectrum difference are used as descriptors for matching the evaluated heartbeat with QRS templates. The performance of the classifiers was tested with the MIT-BIH database. The achieved sensitivity and specificity are 98.4% and 98.86%, respectively.

Fast real time detection of pathological cardiac events was developed by Iliev et al. [18]. It implements QRS detection, inter-beat RR-intervals analysis, QRS waveform evaluation and a decision-tree beat classifier. The amplitude-temporal distribution of the successive QRS pattern waveforms are dynamically accumulated in histogram matrix. The pilot version of the method was developed in MATLAB environment and tested with internationally recognized ECG databases. The obtained sensitivity and positive predictivity with the MIT-BIH database is above 99%.

Algorithms investigating simultaneously more than one ECG lead have some advantages in detection of atypical complexes, although the choice of conjunction or disjunction approach to the candidates detected in different leads is not simple. A sophisticated solution was proposed by Christov [7], who operates with unsigned (absolute) signal values to overcome the opposite in sign deflections of some multi-lead complexes.

On the other hand, the beat detection in single channel ECG signal is very often suitable especially for processing of stand-alone monitors, event recorders for home use, etc.

The majority of the authors do not discuss what kind of maximum time-delay between the detected beats and the corresponding annotation marks is accepted as adequate for exact association of the analyzed beats into the class of true positive.

This short review suggests a presence of enormous number of QRS detection algorithms that implicitly proves the impossibility of building such ideal detector that could totally cover the variety of all encountered shapes of ventricular depolarization. Generally, the studies on the QRS detection are more than ectopic beats classification.

The aim of this study is to develop a very fast procedure for accurate QRS detection in long term ECG recordings and subsequent discrimination of the complexes in normal and ectopic beats.

Material and methodology

The algorithm for ventricular beat recognition was elaborated, tested and assessed with the widely accepted AHA and MIT-BIH databases. The algorithm includes two branches:

1) detection of QRS complexes, and
2) discrimination between normal and ectopic beats.

The two channels of the ECG recordings are processing in parallel.

The accepted strategy consists of processing the ventricular beats consecutively at two levels since in this way the accuracy obtained is higher than the direct detection of normal QRS complexes and ectopic beats. It is very important to eliminate at the first level the high and sharp T waves and even some P waves. Here very often ectopic beats are detected too. They are specified at the second level where additional criteria for ectopic beats investigation are applied over limited epochs of the ECG signals.

Detection of QRS complexes: description of the method and performance evaluation

This branch of the algorithm consists of the following steps: isoelectric line extraction; suppression of high frequency noise and artefacts; fist derivative calculation with optimally reduced sampling rate (SR); determination of the threshold for QRS investigation; parameter specification of the dominant QRS complex; segmentation of the analyzed recording; discovery of erroneously selected candidates.

The signal isoelectric line $iso(n)$, which is usually accepted to be very near to the physiological base line, is obtained using low-pass IIR filter type Butterword, presented by the general difference equation

$$iso[n] = \frac{1}{a_0}\left(\sum_{i=0}^{m} b_i x[n-i] - \sum_{j=1}^{k} a_j [n-j]\right) \quad (1)$$

Here n is the filtered sample, a_0, b_i and a_i are coefficients, m and k stand for the number of processed samples of both filter sections and x represent non-filtered samples.

The implemented version is a fast operating two-component recursive second order low-pass filter with common cut-off at 0.6 Hz.

The isoelectric line *iso*(*n*) is used further on for amplitude analysis of the QRS complexes and polarity determination of their local extremums.

Good performance of applying the filter on signal with considerable drift due to bad electrode-to-skin contact may be observed in Fig. 1. The extracted isoelectric line is red colored.

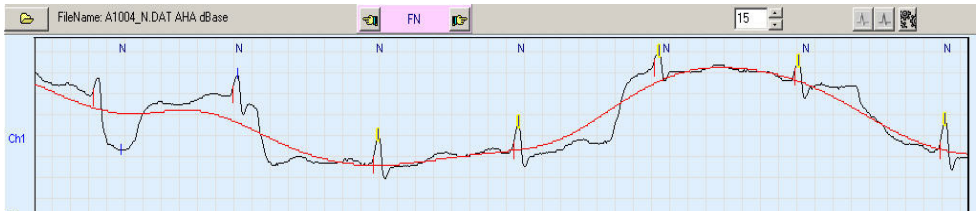

Fig. 1 Isoelectric line extraction from AHA 1004 recording

Artefacts and high frequency noises, which are normally presented in the input ECG signals, are suppressed by a second low-pass filter with the same structure and 15 Hz cut-off.

The first derivative is obtained taking in consideration the analog-to-digital conversion (ADC) parameters and the time properties of the ECG signals. The derivative function with respect to the time is generally given by the equation

$$v(t) = \frac{\Delta y(t)}{\Delta t}, \tag{2}$$

which becomes

$$v(n) = y(n) - y(n+k) \tag{2-1}$$

after ADC. Here n is the ongoing signal sample, k stands for the sample number delimiting the time interval $T_s = kt_{is}$, and t_{is} is the inter-sample distance. The effect of the first differences (2-1) can be enhanced by the expression

$$v(n) = \left(y(n) - y(n+k)\right)^2, \tag{2-2}$$

which is a relevant index of the ECG signal steepness presented by unsigned values.

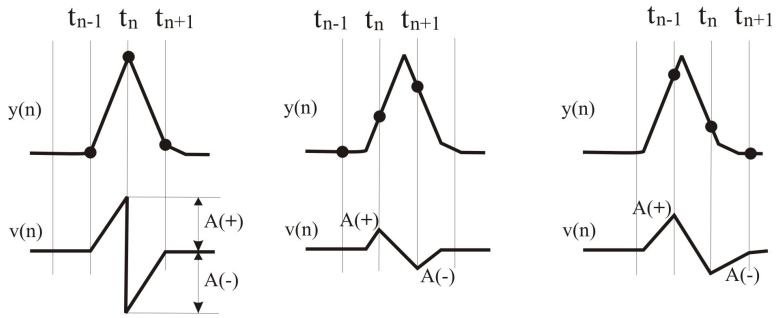

Fig. 2 Examples with time interval $T_s = t_{n-1} - t_{n+1}$ used for obtaining the derivative of QRS complexes

This approach enables the examination of such lowest re-sampling rate (highest k) that suppresses the high-frequency noise components, keeping in the same time the maximum derivative amplitude even in case of short QRS complexes.

Theoretically, a time interval T_s with $k = 2$ inter-sample distances (3 consecutive samples) may fix the polarity change of the QRS derivative if T_s covers the length of the possibly shortest QRS (Fig. 2a).

However, the hit of the maximum amplitude of $v(n)$ needs both strongly periodical ECG signal and accurate synchronization between the first sample of the time interval T_s and the onset of the QRS complex that can be encountered very accidentally in practice. The realistic cases are shown in Figs. 2b and 2c. They suggest the necessity of higher value of k to preserve the maximum amplitude of $v(n)$. On the other hand, if the original SR of the signal remains unchanged, all $v(n)$ amplitudes will go down since the shorter inter-sample distance leads to smaller signal changes.

Our experiments showed the re-sampling rate of 64 Hz (t_{is} = 15.6 ms) as convenient for first derivative processing. This is a good compromise providing for both peaks and steepness preservation. The values of k further used are $k = 4$ for AHA database (SR = 250 Hz; t_{is} = 4 ms) and $k = 6$ for MIT-BIH database (SR = 360 Hz; t_{is} = 2.78 ms). The next Fig. 3 illustrates the advantage of re-sampling with $T' = 4\ t_{is}$ (second trace) comparing to the lower derivative amplitude obtained by $T' = t_{is}$ (fourth trace). The processed signal is AHA 2008 (t_{is} = 4 ms). The red (second and forth) traces show the detected peaks related to the ventricular beats.

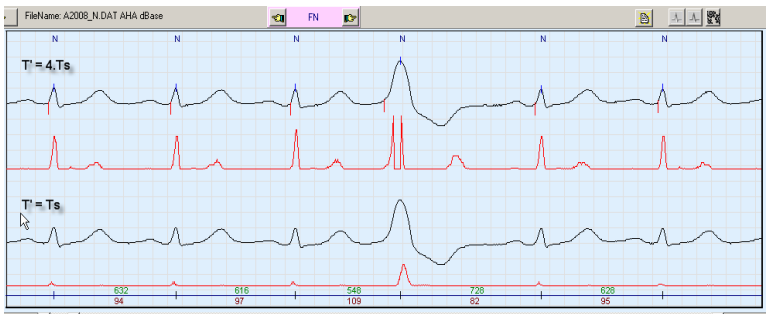

Fig. 3 Results with $T' = 4\ t_{is}$ and $T' = t_{is}$ used for $v(n)$ processing of AHA 2008 recording

The encountered local maximums are collected into one-dimensional accumulator $Acc[i]$ type integer with length "M". The number of cells corresponds to the possible values of amplitudes detected around a complex. The cell size and the length of accumulator comply with the ADC resolution.

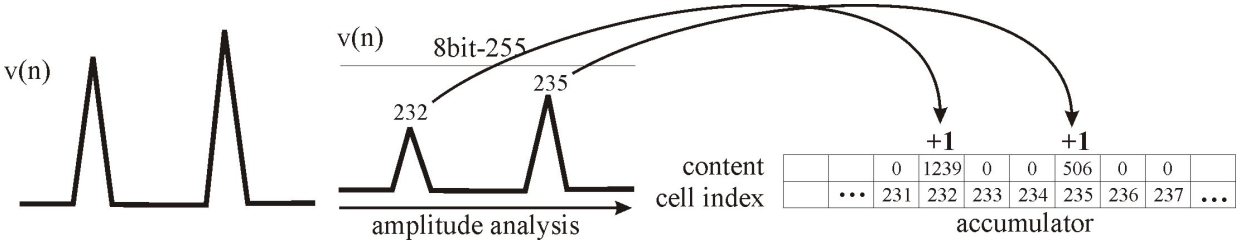

Fig. 4 Processing of encountered local maximums in $v(n)$

Each discovered maximum increments the content of that cell that has index coinciding with the amplitude value. The procedure is illustrated in Fig. 4 by synthesized signal consisting of two peaks, which are re-sampled, differentiated and scaled with ADC size equal to 2^8. The two arrows mark the increment of the number of peaks with relative amplitudes of 232 and 235.

The accumulator content is used for calculation of the threshold L_{thr}, representing the mean value of M detected peak amplitudes.

$$L_{thr} = \frac{\sum_{i=0}^{M} Acc[i]i}{\sum_{i=0}^{M} Acc[i]} \tag{3}$$

Then 50 ms intervals surrounding all derivative amplitudes $v(n) > L_{thr}$ are defined and examined for local maximums that are assumed to be QRS candidates. They are further confirmed by juxtaposing to dominant QRS complex *DQRS,* which is investigated in the analyzed ECG signal. The procedure is similar to that applied for the L_{thr} determination, except for the accumulator $Acc[255][H]$, which is two-dimensional with area sizes of 255 rows and H columns. The borders of the analyzed windows are set at $\pm H/2$ samples on both sides of the current QRS candidate. Here H is equal to 80 for AHA database и 120 for MIT-BIH database that corresponds to an interval length of 320 ms. The dominant complex is presented by the maximum values *DQRS* recorded in the accumulator columns

$$DQRS = \max(Acc[0\text{-}255][q]),\ q = 0, 1, \ldots, H \tag{4}$$

Its accuracy depends on the number of the processed QRS candidates that usually may be reasonably reduced.

Sometimes the amplitude of the QRS complexes in long term ECG recordings varies considerably and the comparison of their amplitudes with the threshold L_{thr} defined by Eq. (3) will introduce significant errors. In such cases the signal has to be segmented into shorted epochs with local thresholds L_{seg}. The QRS amplitude variation is assessed by averaged amplitudes avA_{QRS} calculated over k sequences of complexes.

$$avA_{QRS}(k) = \frac{\sum_{i=1}^{10} A_{(k-1)10+i}}{10} \tag{5}$$

Here $k = (1, 2, ..., n/10)$ and n is the number of all discovered complexes in the recording. For the third signal interval $k = 3$, the avA_{QRS} becomes

$$avA_{QRS}(3) = \frac{\sum_{i=1}^{10} A_{20+i}}{10}$$

Relative deviation between the maximum and the minimum avA_{QRS} that exceeds 30% is accepted as criterion for segmentation. Alternative faster solution consists of unconditional L_{seg} calculation for every epoch of 60 QRS complexes.

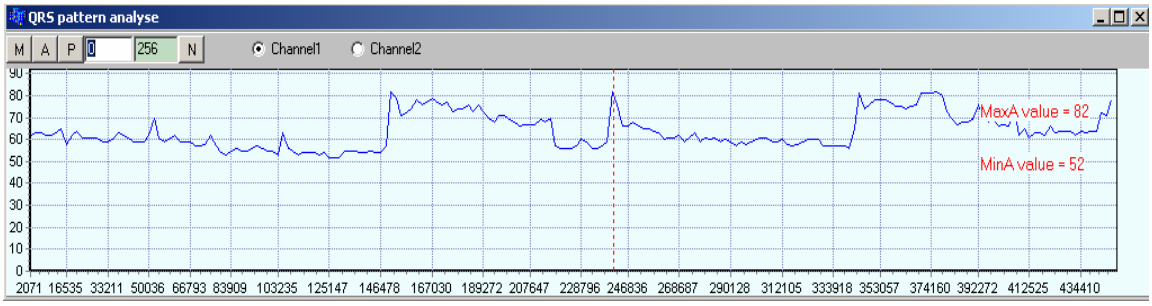

Fig. 5 AHA 1006 recording, channel 1, needing segmentation

Recording needing segmentation is presented in Fig. 5, while Fig. 6 illustrates stable QRS amplitudes.

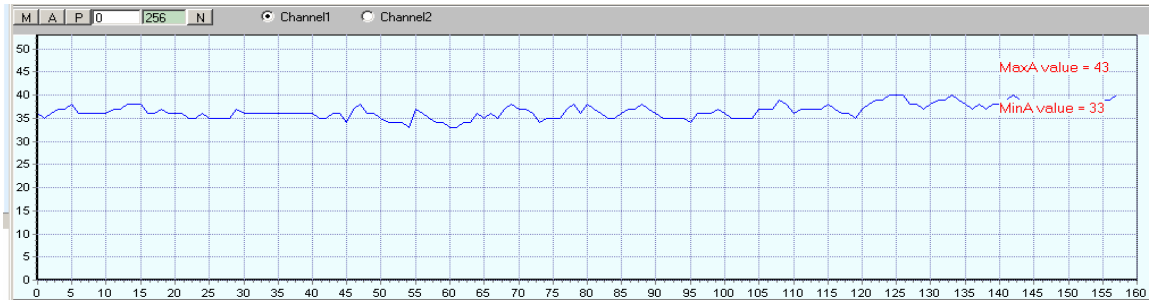

Fig. 6 Relatively stable QRS amplitude – channel 1 of MIT-BIH 100 recording

The detection of QRS complexes ends with checking for erroneously selected candidates. Sometimes the digital filtration is not able to sufficiently suppress all types of noise. Therefore, the detected QRS complexes are subjected to additional processing based on the number and the amplitude of the peaks encountered within a window located around the already marked complexes. To speed up the algorithm, this procedure is applied only on epochs with such noise threshold calculated by Eq. (3) that is higher than 1/3 of the *DQRS* amplitude.

The reached sensitivity and specificity with AHA and MIT-BIH databases are ***Se*** = 99.71%; ***Sp*** = 99.66% and ***Se*** = 96.74%; ***Sp*** = 97.21%, respectively. The allowed deviation between the detected beats and the corresponding annotations is ±30 ms.

Detection of ectopic beats: considerations and approaches

This branch of the algorithm includes determination of individual dominant QRS complexes in segmented epochs; selection of sinus QRS complexes; creation of sinus QRS patterns; investigation of ectopic beats (EB).

The individual dominant QRS complexes *RQRS*(*k*) for *k* segmented epochs are calculated according to Eq. (4) and processed by the averaging filter

$$RQRS(k) = \frac{\sum_{i=n}^{i=n+L} Acc(k)_i}{L} \quad (6)$$

Here $Acc(k)$ is the accumulator used for segment k, n is the ongoing index of the analyzed signal; $L = 5$ for AHA recordings, and $L = 7$ for MIT-BIH recordings. The obtained $RQRS(k)$ are further assigned as reference complexes.

The marked in the first branch *QRS* complexes are subjected to correlation analysis for selection of sinus beats. Although the complexity of the method, the procedure is going fast as it is applied on a few of samples. First at all, the complexes with compensatory pause

$$T_{QRSnQRS(n+1)} \geq 2T_{QRS(n-1)QRSn} \quad (7)$$

are neglected. Here $T_{QRSnQRS(n+1)}$ and $T_{QRS(n-1)QRSn}$ represent the intervals between two consecutive beats.

Then, a scaling coefficient k_M for investigating the remaining complexes is computed

$$k_M = \frac{k_{patMAX}}{k_{sigMAX}} \quad (8)$$

Here

$$k_{patMAX} = \max(RQRS'[n]^2), \; n = (0 \div 79) \quad (9)$$

stands for the maximum of the k-th squared reference derivative *RQRS'* and

$$k_{sigMAX} = \max(RQRS'[n].QRS'[n+q]), \; q = (0 \div 79) \quad (10)$$

represents the maximum among the derivatives of the *RQRS'* samples, multiplied with the shifted by q positions derivative samples of the analyzed QRS complex; n is the current derivative index.

If even only one absolute difference between corresponding sample couples of $QRS(k)$ and $RQRS(k)$ becomes

$$abs(k_M * QRS[k, n] - RQRS[k, n]) > 0.25 \; RQRS[k, n] \quad (11)$$

then this $QRS(k)$ is not sinus complex and belongs to the set of potential EB.

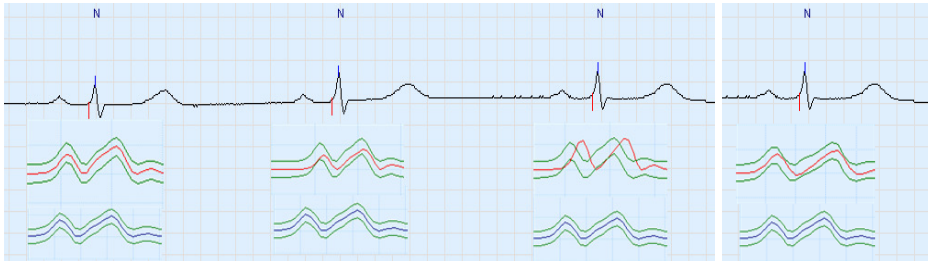

a) b)

Fig. 7 Correlation analysis of similar QRS complexes: a) without k_M; b) with k_M

The contribution of k_M to the accurate selection of sinus complexes may be appreciated in Fig. 7. Three consecutive evidently normal beats are subjected to correlation analysis without scaling coefficient (Fig. 7a). The third one is erroneously classified as potential EB that does not happen when k_M is used (Fig. 7b). Here the red traces (second lines of the middle part of the Figures) stand for the first derivatives of the examined complexes. The blue traces (second lines of the low part of the Figures) depict the reference complexes. The green traces (first and third lines encountering the complexes) mark the tolerances.

The sinus dominant complexes called templates $T_{te}[k]$ are defined by width, steepness and amplitude extracted from the set of sinus QRS complexes $\sin QRS[k]$, $k = 0 \div 79$. The width W_{te} is measured over the central segment of $Acc(k)$ that is surrounded by isoelectric lines. They are recognized by the following 5 consecutive sample differences that do not exceed 2 bits

$$\begin{aligned} &abs(\sin QRS[k] - \sin QRS[k+1]) < 2 \\ &abs(\sin QRS[k] - \sin QRS[k+2]) < 2 \\ &abs(\sin QRS[k] - \sin QRS[k+3]) < 2 \\ &abs(\sin QRS[k] - \sin QRS[k+4]) < 2 \\ &abs(\sin QRS[k] - \sin QRS[k+5]) < 2 \end{aligned} \quad (12)$$

The steepness S_{te} represents the mean difference of N samples before and N samples after the extremum of the reference complex $\sin QRS[k]$. N equals 5 in case of AHA database recordings and takes the value of 7 for MIT-BIH database. The amplitude A_{te} is the absolute difference between the maximum and the minimum inside $\sin QRS[k]$.

The QRS complexes, detected by the first algorithm branch, are checked for affiliation to the set of EB by correlation analysis on the parameters of the QRS complexes and the corresponding templates (W_{te}, S_{te} and A_{te}). The results obtained in both channels are combined by disjunction function.

Selected cases of correlation analysis applied on both channels of AHA 6009 recording are shown in Fig. 8 in two rows for the first and second channel, respectively. The traces are colored as in Fig. 7. The red rectangles encompass the detected EB (third and fifth in the first row; second, third and fifth in the second row), the green color being used for normal beats.

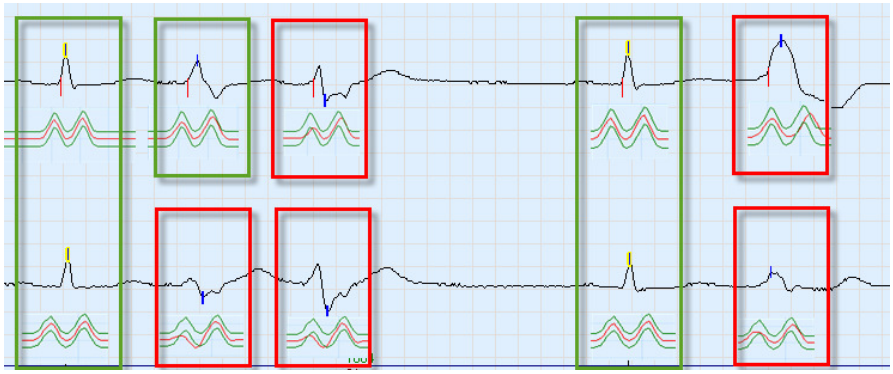

Fig. 8 Selected cases of correlation analysis
applied on both channels of AHA 6009 recording

Results

The discrimination performance between normal and ectopic beats is checked over AHA and MIT-BIH databases. The allowed deviation between the classified beats and the corresponding annotations is again ±30 ms.

The calculated sensitivities and specificities of normal beat and ectopic beat detections are *Se* = 99.71%, *Sp* = 99.66%, *SeEB* = 92.27% and *SpEB* = 94.78% for AHA database; *Se* = 96.74%, *Sp* = 97.21%, *SeEB* = 90.05% and *SpEB* = 86.46% for MIT-BIH database. Table 1 and Table 2 show in detail the results obtained with each of the recordings of both database.

The AHA 8xxx section was neglected during the evaluation of the algorithm accuracy, since it contains ECG signals with ventricular fibrillation. The red highlighted signals AHA 2003 and 5009, MIT-BIH 201, 207 and 232 (with corrupted markers of the events), and MIT-BIH 102, 104 and 217 (files with paced activity) were either not taken in consideration

The first case is illustrated by episode of the AHA 2003 recording (Fig. 9) where the shifted annotation marks are recognized as FN, while the real QRS complexes are qualified as FP. This is done by program especially written for automated checking whether the detected beat positions fall into the window of ±30 ms around the annotated beats.

Table 1. AHA database

dBase AHA	*Se*	*Sp*	*EB*	*True positive*	*False negative*	*False positive*	*SeEB*	*SpEB*
1001	99.88	100	0	0	0	1	0	0
1002	100	100	0	0	0	2	0	0
1003	99.45	99.4	0	0	0	3	0	0
1004	99.93	99.56	0	0	0	6	0	0
1005	99.61	100	0	0	0	169	0	0
1006	100	100	0	0	0	0	0	0
1007	100	100	0	0	0	0	0	0
1008	100	100	0	0	0	0	0	0
1009	95.9	99.97	0	0	0	20	0	0
1010	95.89	98.61	0	0	0	74	0	0
2001	100	100	73	73	0	1	100	98.65

2002	100	100	54	41	13	728	75.93	5.33
2003	85.63	85.41	13	7	6	6	0	0
2004	98.89	99.8	38	35	3	30	92.11	53.85
2005	99.82	100	59	59	0	5	100	92.19
2006	99.94	100	269	269	0	0	100	100
2007	99.91	100	276	275	1	8	99.64	97.17
2008	99.96	100	309	308	1	2	99.68	99.02
2009	100	99.96	144	144	0	0	100	100
2010	99.88	99.96	79	79	0	2	100	97.53
3001	99.95	99.77	26	25	1	14	96.15	64.1
3002	99.97	100	59	58	1	0	98.31	100
3003	100	99.64	35	35	0	6	100	85.37
3004	100	99.73	79	77	2	2	97.47	97.47
3005	100	100	14	7	7	0	50	100
3006	100	100	113	113	0	2	100	98.26
3007	99.96	100	27	26	1	0	96.3	100
3008	99.96	99.92	115	115	0	0	100	100
3009	100	98.55	62	61	1	1	98.39	98.39
3010	99.23	99.76	81	78	3	6	96.3	92.86
4001	99.95	100	441	441	0	0	100	100
4002	99.75	99.92	120	111	9	4	92.5	96.52
4003	100	100	474	473	1	0	99.79	100
4004	99.78	100	109	49	60	0	44.95	100
4005	99.79	99.86	146	142	4	0	97.26	100
4006	99.69	100	156	141	15	7	90.38	95.27
4007	100	99.89	642	619	23	12	96.42	98.1
4008	100	99.73	25	25	0	0	100	100
4009	99.62	98.95	827	822	5	5	99.4	99.4
4010	99.97	100	684	556	128	0	81.29	100
5001	98.45	99.82	235	75	160	0	31.91	100
5002	99.49	100	164	152	12	3	92.68	98.06
5003	99.79	100	4	2	2	0	50	100
5004	99.96	95.25	360	359	1	0	99.72	100
5005	100	99.94	316	314	2	0	99.37	100
5006	99.95	99.95	45	45	0	3	100	93.75
5007	99.97	100	46	46	0	0	100	100
5008	99.84	99.95	35	35	0	0	100	100
5009	74.92	74.71	11	8	3	4	0	0
5010	99.95	99.46	355	353	2	2	99.44	99.44
6001	100	100	46	46	0	0	100	100
6002	99.85	99.95	237	231	6	4	97.47	98.3
6003	99.96	99.96	157	156	1	1	99.36	99.36
6004	99.51	99.96	136	118	18	12	86.76	90.77
6005	98.78	99.87	204	171	33	3	83.82	98.28
6006	99.61	98.13	360	326	34	27	90.56	92.35
6007	99.95	99.08	463	463	0	2	100	99.57
6008	100	100	51	47	4	0	92.16	100
6009	100	99.17	750	748	2	6	99.73	99.2

6010	99.6	94.99	394	382	12	9	96.95	97.7
7001	99.81	100	650	639	11	8	98.31	98.76
7002	99.86	99.91	219	216	3	0	98.63	100
7003	99.92	99.96	170	168	2	8	98.82	95.45
7004	99.53	99.22	42	34	8	5	80.95	87.18
7005	99.79	99.92	168	159	9	0	94.64	100
7006	99.9	99.65	1884	1129	755	216	59.93	83.94
7007	99.91	99.83	93	92	1	4	98.92	95.83
7008	100	100	41	41	0	0	100	100
7009	100	99.79	1638	1624	14	3	99.15	99.82
7010	100	99.89	18	18	0	0	100	100
	99.71	**99.66**					**92.27**	**94.78**

Table 2. MIT-BIH Database

dBase "MIT-BIN"	*Se*	*Sp*	*EB*	*True positive*	*False negative*	*False positive*	*SeEB*	*SpEB*
100	100	100	1	1	0	0	100	100
101	99.79	99.95	0	0	0	2	100	100
102	99.53	97.43	4	2	2	129	0	0
103	100	97.39	0	0	0	63	100	100
104	0	0	2	2	0	609	0	0
105	97.5	98.51	41	38	3	69	92.68	35.51
106	98.33	99.01	520	429	91	3	82.5	99.31
107	99.95	99.94	59	46	13	2	77.97	95.83
108	97.69	98.92	17	12	5	39	70.59	23.53
109	99.92	99.96	38	35	3	1	92.11	97.22
111	99.72	99.95	1	1	0	2	100	33.33
112	99.01	99.96	0	0	0	0	100	100
113	99.56	100	0	0	0	1	100	100
114	99.95	100	43	43	0	18	100	70.49
115	99.8	99.8	0	0	0	9	100	100
116	98.96	99.96	109	107	2	1	98.17	99.07
117	99.93	99.93	0	0	0	0	100	100
118	99.56	100	16	15	1	2	93.75	88.24
119	100	100	444	444	0	1	100	99.78
121	100	100	1	1	0	1	100	50
122	99.92	99.96	0	0	0	0	100	100
123	99.8	100	3	0	3	0	0	100
124	99.57	100	47	34	13	3	72.34	91.89
200	98.6	98.82	826	719	107	113	87.05	86.42
201	0	0	198	6	192	104	0	0
202	99.86	100	19	19	0	3	100	86.36
203	94.89	99.28	444	404	40	334	90.99	54.74
205	99.36	100	71	64	7	0	90.14	100
207	0	0	105	55	50	1758	0	0
208	98.37	99.56	994	906	88	292	91.15	75.63
209	92.17	99.61	1	1	0	7	100	12.5

210	94.62	99.72	194	107	87	10	55.15	91.45
212	99.93	99.96	0	0	0	59	100	100
213	99.85	100	220	215	5	1	97.73	99.54
214	99.48	99.83	256	199	57	9	77.73	95.67
215	98.55	100	164	142	22	1	86.59	99.3
217	96.06	88.04	162	98	64	241	0	0
219	99.66	99.96	64	51	13	0	79.69	100
220	99.9	99.95	0	0	0	0	100	100
221	99.34	99.79	396	369	27	0	93.18	100
222	99.68	99.84	0	0	0	68	100	100
223	96.23	99.36	473	260	213	8	54.97	97.01
228	98.75	100	362	358	4	2	98.9	99.44
230	99.96	100	1	1	0	0	100	100
231	100	100	2	2	0	2	100	50
232	0	0	0	0	0	5	0	0
233	99.68	99.94	831	820	11	9	98.68	98.91
234	99.85	100	3	3	0	0	100	100
	96.74	**97.21**					**90.05**	**86.46**

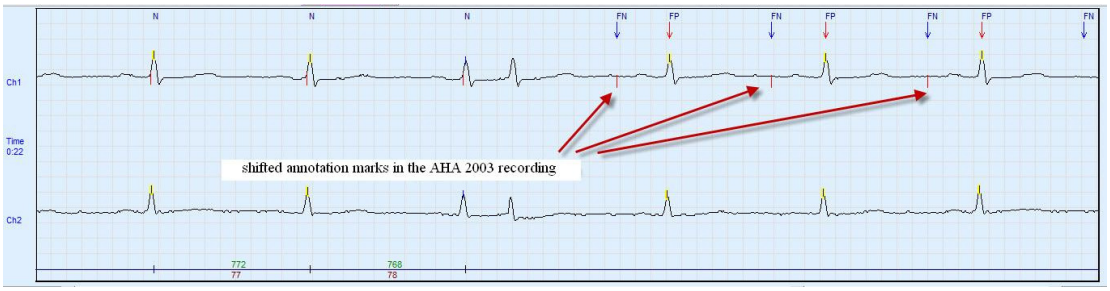

Fig. 9 Shifted annotation mark in the last quarter of the AHA 2003 recording

The next Fig. 10 is selected to show the paced cardiac activity in the above cited recordings of MIT-BIH database.

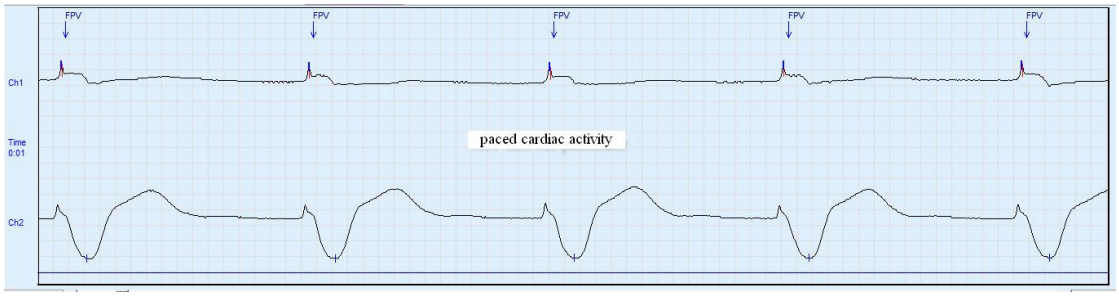

Fig. 10 Example of paced cardiac activity in MIT-BIH 102 recording

Discussion and conclusions

The algorithm for discrimination between normal and ectopic beats in long term recordings consists at first sight of reiterating procedures. Actually, the repeated procedures are applied on the content of limited number of accumulators.

The cut-offs of both low-pass filters enclose frequency band, which differs from that, usually obtained by band-pass filtering within 5÷25 Hz. Thus, the enhanced lower signal components better preserve the shape of the ventricular beats.

The reduced SR used for the signal differentiation contributes to a subsequent processing of free of noise high amplitudes.

The indirect procedure for selection of sinus beats seems too complex but the alternative approach is not possible since the ectopic beats have different shapes.

The program implementing the algorithm is written in C++. The detection and discrimination of sinus and ectopic beats in a 24 hour Holter recording need about 7-8 min. This result is fixed by measuring the time for analysis of AHA database files. Each of them is with duration from 30-33 min and is processed for 7-11 s. Such approach for assessment of the algorithm speed has advantage since the widely accepted databases consist of ECG signals, which are more complex and difficult for processing than the majority of the real 24 hours recordings.

References

1. Afonso V. X., W. J. Tompkins, T. Q. Nguyen, S. Luo (1999). ECG Beat Detection using Filter Banks, IEEE Trans Biomed Eng, 46, 192-202.
2. Arzeno N. M., C.-S. Poon, Z.-D. Deng (2006). Quantitative Analysis of QRS Detection Algorithms based on First Derivative of the ECG, Proc. of 28th IEEE EMBS Annual International Conference, New York, USA, 1788-1791.
3. Arzeno N. M., Z.-D. Deng, C.-S. Poon (2008). Analysis of First-derivative based QRS Detection Algorithms, IEEE Trans Biomed Eng, 55(2), 478-484, doi: 10.1109/TBME.2007.912658.
4. Bartolo A., B. D. Clymer, R. C. Burgess, J. P. Turnbull, J. A. Golish, M. C. Perry (2001). An Arrhythmia Detector and Heart Rate Estimator for Overnight Polysomnography Studies, IEEE Trans Biomed Eng, 48(5), 513-521.
5. Benitez D., P. A. Gaydecki, A. Zaidi, A. P. Fitzpatrick (2001). The Use of Hilbert Transform in ECG Signal Analysis, Comp in Biology and Medicine, 31, 399-406.
6. Chen H. C., S. W. Chen (2003). A Moving Average based Filtering System with its Application to Real-time QRS Detection, Comput Cardiol, 30, 585-588.
7. Christov I. I. (2004). Real Time Electrocardiogram QRS Detection using Combined Adaptive Threshold, BioMed Eng OnLine, 3(28), doi:10.1186/1475-925X-3-28.
8. Christov I. I. (2007) Assessment of the Performance of the Adaptive Thresholding Algorithm for QRS Detection with the Use of AHA Database, International Journal Bioautomation, 6, 27-37.
9. Das S., M. Chakraborty (2011). QRS Detection Algorithm using Savitzky-Golay Filter, Proc. of Int. Joint Colloquium on Emerging Technologies in Computer Electrical and Mechanical, 56-59, doi:02.CEM.2011.01.550.
10. Darrington J. (2006). Towards Real Time QRS Detection: A Fast Method using Minimal Pre-processing, Biomedical Signal Processing and Control, 1, 169-176.
11. Dinh H. A. N., D. K. Kumar, N. D. Pah, P. Burton (2001). Wavelets for QRS Detection, Proc. of 23rd IEEE EMBS Int. Conference, 1883-1887.

12. Dotsinsky I., I. Christov (1997). Detection of QRS Complexes and Ventricular Ectopic Beats in the Electrocardiogram, International Scientific Colloquium, Ilmenau, Band 2, 99-103.
13. Dotsinsky I. A., T. V. Stoyanov (2004). Ventricular Beat Detection in Single Channel Electrocardiogram, BioMed Eng OnLine, 3:3, http://www.biomedical-engineering-online.com/content/3/1/3.
14. Engin M. (2004). ECG Beat Classification using Neuro-fuzzy Network, Pat Rec Letters, 25, 1715-1722.
15. Fernandez J., M. Harris, C. Meyer (2005). Combining Algorithms in Automatic Detection of R-peaks in ECG Signals, Proc. of the 18th IEEE Symposium on Computer-based Medical Systems, 297-302.
16. Haiying Zhou, Kun-Mean Hou, Decheng Zou (2009). Real-time Automatic ECG Diagnosis Method Dedicated to Pervasive Cardiac Care Wireless Sensor Network, 1, 276-283, doi:10.4236/wsn.2009.14034, http://www.scirp.org/journal/wsn
17. Harikumar R., S. N. Shivappriya (2011). Analysis of QRS Detection Algorithm for Cardiac Abnormalities – A Review, International Journal of Soft Computing and Engineering, 1(5).
18. Iliev I., V. Krasteva, S. Tabakov (2007). Real-time Detection of Pathological Cardiac Events in the Electrocardiogram, Physiol Meas, 28, 259-276, doi:10.1088/0967-3334/28/3/003.
19. Kadambe S., R. Murray, G. F. Boudreaux-Bartels (1999). Wavelet Transform-based QRS Complex Detector, IEEE Trans Biomed Eng, 46, 838-848.
20. Kohler B.-U., C. Hennig, R. Orlgmeister (2002). The Principles of Software QRS Detection, IEEE Trans Eng Med Biol Mag, 21(1), 42-57.
21. Köhler B.-U., C. Hennig, R. Orlgmeister (2003). QRS Detection using Zero Crossing Counts, Progress in Biomedical Research, 8(3), 138-145.
22. Krasteva V., I. Jekova (2007). A QRS Template Matching for Recognition of Ventricular Ectopic Beats, Annals of Biomedical Engineering, 35(12), 2065-2076, doi:10.1007/s10439-007-9368-9.
23. Mehta S. S., N. S. Lingayat (2007). Comparative Study of QRS Detection in Single Lead and 12-lead ECG based on Entropy and Combined Entropy Criteria using Support Vector Machine, Journal of Theoretical and Applied Information Technology, 8-18.
24. MIT-BIH Arrythmia Database, 2nd edition. Cambridge, MA (1992): Massachusetts Institute of Technology, Biomedical Engineering Center, available from: URL: http://www.physionet.org/physiobank/database/html/mitdbdir/mitdbdir.htm
25. Paoletti M., C. Marchesi (2006). Discovering Dangerous Patterns in Long-term Ambulatory ECG Recordings using a Fast QRS Detection Algorithm and Explorative Data Analysis, Comp Methods and Progs in Biomed, 82, 20-30.
26. Pant S., A. K. Wadhwani (2011). A Real Time QRS Detection System Used Error Back Propagation Neural Network, Int J of Electrical, Electronics and Computer Engineering, 1(1), 48-54.
27. Poli R., S. Cagnoni, G. Valli (1995). Genetic Design of Optimum Linear and Nonlinear QRS Detectors, IEEE Trans Biomed Eng, 42, 1137-1141.
28. Portet F., A. I. Hernández, G. Carrault (2005). Evaluation of Real-time QRS Detection Algorithms in Variable Contexts, Med Biol Eng Comput, 43(3), 381-387.
29. Ruha A., S. Sallinen, S. Nissilä (1997). A Real-time Microprocessor QRS Detector System with a 1-ms Timing Accuracy for the Measurement of Ambulatory HRV, IEEE Transactions on Biomedical Engineering, 44(3), 159-167.

30. Sasikala P., R. S. D. Wahidabanu (2010). Robust R Peak and QRS Detection in Electrocardiogram using Wavelet Transform, International Journal of Advanced Computer Science and Applications, 1(6), 48-53.
31. Saxena S. C., V. Kumar, S. T. Hamde (2002). Feature Extraction from ECG Signals using Wavelet Transform for Disease Diagnostics, International Journal of System Science, 33, 1073-1085.
32. Saurabh Pal, Madhuchhanda Mitra (2012). Empirical Mode Decomposition based ECG Enhancement and QRS Detection, Computers in Biology and Medicine, 42, 83-92.
33. Sumathi S., M. Y. Sanavullah (2009). Comparative Study of QRS Complex Detection in ECG based on Discrete Wavelet Transform, International Journal of Recent Trends in Engineering, 2(5), 273-277.
34. Sun Y., K. L. Chan, S. M. Krishnan (2005). Characteristic Wave Detection in ECG Signal using Morphological Transform, BMC Cardiovascular Disorders, 5(28), doi:10.1186/1471-2261-5-28, http://www.biomedcentral.com/1471-2261/5/28.
35. Szi-Wen Chen, Hsiao-Chen Chen, Hsiao-Lung Chan (2006). A Real-time QRS Detection Method based on Moving-averaging Incorporating with Wavelet Denoising, Computer Methods and Programs in Biomedicine, 82, 187-195.
36. Trahanias P. E. (1993). An Approach to QRS Complex Detection using Mathematical Morphology, IEEE Trans Biomed Eng, 40(2), 201-205.
37. Xue Q., Y. H. Hu, W. J. Tompkins (1992). Neural-network-based Adaptive Matched Filtering for QRS Detection, IEEE Trans Biomed Eng, 39, 317-329.

Stoyan Tanev
E-mail: spsbyte@space.bas.bg

Stoyan Tanev is Head of Department "Aerospace Techniques and Technology" in the Institute of Space Research and Technology, Bulgarian Academy of Science. He received M.Sc. degree (1985) in the Air Force Academy – Dolna Mitropolia with qualification engineer on radio control and navigation of the flights. He specialized "Onboard computers systems" in the Space Research Institute. He has over 30 publications. He was team leader in development of most than 40 scientific apparatuses, 11 of them in the area of medicine. Leading engineer in two space projects. Current interests are in the field of digital signals processing and real time signals processing.